FRACTURE MECHANICS OF PLATE DEBONDING: EXPERIMENTAL VALIDATION

Mithila ACHINTHA Chris BURGOYNE

Department of Engineering, University of Cambridge, UK

Keywords: Branson's model, energy release rate, fracture energy, plate debonding

1 INTRODUCTION

Premature plate debonding hampers the efficient use of externally bonded FRP plates for flexural strengthening of concrete beams. Existing research mostly concentrates on finite element (FE) modelling of the concrete–FRP interface but such analyses are of dubious validity because they require far more details than will ever be available for the interface [1,2]. A fracture-mechanics-based plate debonding model has been developed by the authors [1,2,3]; since detailed stress analysis of concrete is unattainable the model is based on the global energy balance of the system. Flaws will inevitability be present in the vicinity of the interface; the model investigates the energy balance when such a flaw propagates. The energy released when the crack extends (G_R) is compared with the interface fracture energy required to create the new surfaces G_F: If $G_R \geq G_F$ the crack will extend causing debonding.

Determination of both G_R and G_F associated with crack extension is not trivial because of the unknowable microstructure of concrete. The early work of the present study developed methods to find both parameters to accuracies sufficient for practical purposes [1-3]. A modified version of Branson's model, which takes account of the effects caused by the axial force in the FRP, has been developed for the moment–curvature and subsequent G_R analyses, while G_F has been determined according to the actual fracture mechanism that takes place in the interface.

This paper presents comparisons with a variety of plate debonding test data (including steel plate bonded beams) reported in the literature and shows that the present model can correctly determine both the failure load and the debonding mode. Only simply-supported beams, without additional plate end anchors, under short-term monotonic loads are considered here, but the model could be extended to analyse more complex practical problems.

2 APPLICATION OF THE MODEL

The present analytical model answers the question "will this existing interface crack extend?" for both modes of debonding (plate-end-debonding into the beam and midspan-debonding towards the nearest beam end). Both G_R and G_F are evaluated for assumed interface crack lengths and locations and then the critical state is determined when G_R equals G_F. The application of the model, together with the qualitative advantages over existing plate debonding analyses were presented in [2].

The experimental evidence confirms that in most practical cases concrete is most liable to fail than the adhesive, and also the debonding takes place locally by opening of the existing debonding crack tip. Hence G_F must be the Mode I (crack opening mode) fracture energy of the concrete ($G_{C\mathrm{I}}$) [3]. The model can also accurately analyse failures in a weak adhesive.

3 OVERVIEW OF METHOD ADOPTED IN THE COMPARISONS

Comparisons between the test data and the present model have been made for some of the test specimens found from the literature covering both plate end and midspan debonding failures. Due to space constraints, only a few such comparisons are shown here; similar results have been obtained for other test data (detail of the full database of comparisons is presented elsewhere [4]).

Because there is a considerable variation in fracture effects, for any chosen example the G_R corresponding to the reported failure load, and loads 10% higher and lower loads are compared with $G_{C\mathrm{I}}$ with a 10% higher and lower variation. $G_{C\mathrm{I}}$ is selected by taking account of the aggregate size and type, and strength of the concrete (i.e. the water:cement ratio); a detailed description on the selection of $G_{C\mathrm{I}}$ is presented in [3].

All the beams analysed here were tested as simply-supported beams under 4-point bending with equal shear spans. Any missing data in the original publications have been replaced by assumed values: however, normally only the less significant thickness and the shear modulus of the adhesive are absent in the original publications. When available, load–deflection curves of both strengthened and control beams were validated prior to the debonding analysis.

4 PLATE END DEBONDING

It has shown that the distance to the plate curtailment position from the beam support (L_0) governs plate end (PE) debonding [2]. Thus, G_R corresponding to a given combination of L_0 and P (applied load) must be investigated as discussed in [2].

4.1 Effective plate end location

It has been observed that PE debonding initiates from a shear crack that develops at the plate end and propagates towards the internal tension steel (e.g. [5]). This development causes partial separation of the FRP resulting in an interface crack in the plate end vicinity (Figure 1(a)). So, the "effective plate end location" (L_{0_eff}) is now located at some distance beyond the actual L_0. The location of L_{0_eff} depends on how far the initial shear crack develops prior to the initiation of critical debonding. If the associated G_R is sufficient to cause debonding then the propagation will start just after the formation of the shear crack, else the critical state may only be attained after the initial crack reaches the tension steel. With the assumption of 45^0 propagation of the shear crack it is contended that the additional ineffective length of the FRP just before critical debonding to be between 0 and c (where c is the cover to the tension steel bars).

4.2 Plate end debonding initiates from intermediate shear cracks

When the plate is curtailed near the beam support the critical zone is located in a low energy region and hence any interface crack that develops in the plate end vicinity is associated with smaller G_R values in comparison to G_{Cl} [4]. Thus, no PE debonding is expected here. However, shear cracks are inevitable in the beam span, especially if the shear provision of the beam remains that of the original unstrengthened beam. Widening of shear cracks produces high stress concentrations and the subsequent diagonal microcracks can cause the separation of the narrow potion of the plate towards the plate end (Figure 1(b)). The peeled plate carries no force and hence the L_{0_eff} is now located at the bottom of the critical shear crack; debonding analysis can now be performed by taking L_{0_eff} as the plate curtailment location, which is now in a relatively high energy zone.

5 COMPARISONS WITH TESTS: PLATE END DEBONDING

5.1 Plate end interface crack induced debonding

The L_{0_eff} which triggers debonding is expected to be a short distance (< cover c) away from the actual L_0. So, the G_R values corresponding to the L_{0_eff} range within two cover depths of the actual L_0 are investigated here.

Figure 2 (solid lines) shows the variation in G_R against L_{0_eff} of the 2 beam pairs selected from the study of Fanning & Kelly [5]. G_{Cl} is assumed to be 0.15 N/mm for the 20 mm crushed aggregates used in the tests [3]. The figure shows that the reported debonding loads and failure modes of the 2 beam pairs match the test results if L_{0_eff} is between 5 and 10 mm higher than the actual L_0. Note that the cover was 30 mm.

The same figure also shows that at the observed failure loads any L_{0_eff} shorter than actual L_0 does not cause PE debonding: this further validates the present analysis since a critical interface crack with a positive magnitude is required to trigger debonding. Furthermore, the figure shows that for both beam pairs the load levels 10% higher or lower load than the observed failure load (broken lines) are too strong or too weak respectively to cause PE debonding near the actual L_0. The analysis of other test data also shows similar results validating the present analysis [4].

5.2 Intermediate shear crack induced debonding

Beam SP-T6 tested by Mohamed Ali et al. [6] strengthened with a steel plate curtailed at 50 mm from the beam support, but the beam failed by PE debonding that resulted from widening of a shear crack located 350 mm away from the beam end. 10 mm crushed aggregate was used in the concrete so G_{Cl} is assumed to be 0.1 N/mm [3]. Figure 3 shows the G_R vs L_{0_eff} plot corresponding to the actual plate end vicinity (L_0 = 50 mm); the low values for G_R demonstrate the inability to develop a critical

interface crack there. The plot also shows that in the vicinity of the observed shear crack (L_{0_eff} = 350 mm) G_R is equal to G_{Cl}, which is in accordance with the reported failure

5.3 Premature adhesive failures

The use of a weaker adhesive or poor workmanship can cause premature adhesive failure, and is demonstrated using beams B2 and B3 tested by Quantrill et al. [7]. The failure of B2 was reported as "plate and concrete cover separation" – i.e. failure in the concrete. The "plate separation" – i.e. the separation of the FRP without affecting the interface concrete (an adhesive failure) was quoted for B3. 10 mm rounded aggregate was used, so, G_{C1} is assumed to be 0.07 N/mm [3]. Figure 4 shows G_R vs L_{0_eff} plot at the reported failure loads of both beams within the expected L_{0_eff} range of 70–100 mm. The figure shows that the expected G_R for B2 at L_{0_eff} of 85 mm matches G_{Cl}, justifying the reported failure load. But, G_R of only about 50% of G_{Cl} is shown for B3 at the same critical L_{0_eff} vicinity: so, interface concrete failure is not justified. The fracture energy of the adhesive is not known but must have been lower than that of the concrete. The present analysis however accurately distinguishes premature adhesive failures from the interface concrete failure.

6 MIDSPAN DEBONDING

The analysis of midspan (MS) debonding is more complicated; both the length of the existing debonding crack (l_d) and the crack location in the beam span must be investigated. The earlier analytical work of the present study [2, 4] has shown that in simply supported beams MS debonding propagates towards the beam end justifying the test observations. It has also shown that short interface cracks (often less than 10 mm long) develop at high moment zones can cause debonding in contrast to the requirement of much longer cracks at low moment zones. As is confirmed by the results shown here, mostly short cracks developed at higher applied loads (above 90% of the ultimate capacity) triggered MS debonding in the test beams. This behaviour is different to the strong influence of the plate curtailment location on PE debonding load [2,4].

7 COMPARISONS WITH TESTS: MIDSPAN DEBONDING

7.1 Critical Flexural Crack Induced MS Debonding

In most 4-point bending tests MS debonding initiates from the widening of a critical flexural crack, located in one of the shear spans in the close vicinity of the load point (the highest energy zone). The exact location of the critical crack is a prerequisite in the analysis; the assumption of a half beam depth away from the load point gives accurate comparisons with test data [4]. Note that the choice of this offset from the load point also justifies the section analysis adopted in the present work [1,2].

Solid lines in Figure 5 shows G_R corresponding to the reported failure load (98% of the ultimate) for a fracture propagating from an internal crack at a half-beam depth away from the load point of a beam (B1) tested by Garden et al. [8]. G_{Cl} of the high strength mix with 10 mm crushed aggregate is assumed to be 0.12 N/mm. The figure shows a critical crack of length (l_{d_cr}) 4.8 mm causes debonding here. Debonded lengths like this may well be present, and undetectable, in many practical applications. The predicted l_{d_cr} compares well with the relative vertical displacement between the two surfaces of the critical crack (2 mm) observed in the tests just before debonding [8].

7.2 Critical Flexural/Shear Crack Induced MS Debonding

An interface flaw that can be developed at the base of a flexural/shear crack is often longer than that due to a flexural crack because of the relatively larger vertical displacements between the two crack surfaces associated with the former. So, when no critical interface cracks are developed at the highest moment zone, debonding can be caused by a relatively longer flaw initiated at a flexural/shear crack (at a relatively low energy zone). This mode of MS debonding is however not common but can be expected in beams with low span: depth ratios.

Dashed lines in Figure 5 shows G_R vs l_d plot for a short beam (B2) (with span: depth ratio of 3) tested in the same study [8] at the failure load (92% of the ultimate). Here, debonding initiated from a flexural/shear crack and the offset of the crack (from the load point) has been scaled from a figure in the original reference. The figure shows that l_{d_cr} of 2.2 mm causes debonding at the reported failure load. The depth of this beam (h) was half that of the former, giving the same l_{d_cr}: h ratio. Similar results have been obtained for the other test specimens [4].

8 CONCLUSIONS

The comparisons presented herein validate the fracture mechanics based plate debonding model developed in the present study. This will obviate the need for finite element analyses to be used in situations where there is an infinite stress concentration and where the exact details of the interface geometry and properties are unknowable. The model successfully employs the critical interface crack concept, but it does not show how the critical shear crack distribution evolves which should be the subject of future research.

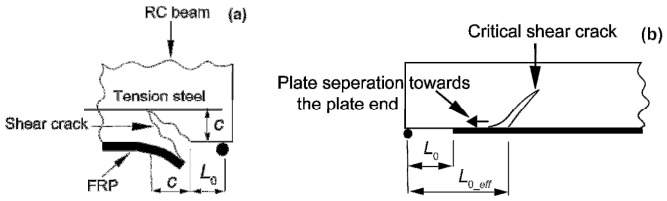

Fig.1 L_{0_eff} for (a) plate-end-interfacial crack (b) Shear-crack-induced debonding

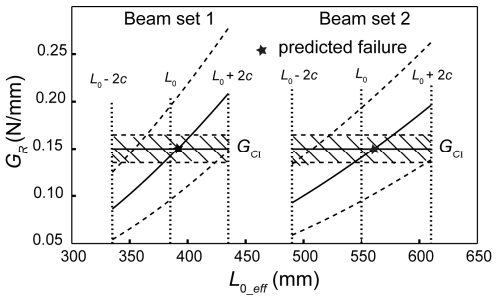

Fig.2 $G_R - L_{0\_eff}$ plot for Fanning & Kelly [5] two beam sets

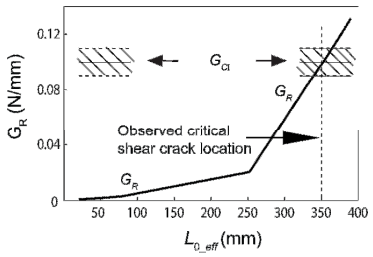

Fig. 3 Shear-crack-induced PE debonding [6]

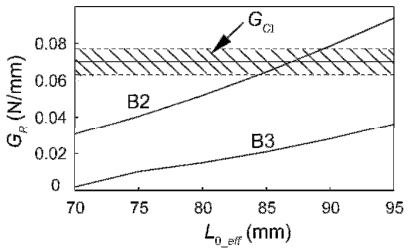

Fig. 4 Concrete failure against premature adhesive failure

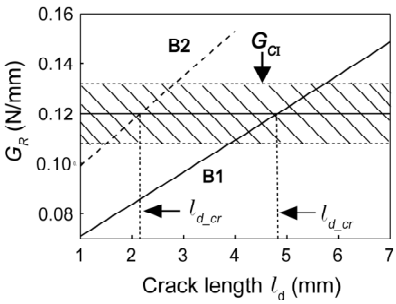

Fig. 5 Critical crack lengths for midspan debonding

REFERENCES

[1] Achintha, P.M.M. and Burgoyne, C.J., "Moment–Curvature and Strain Energy of Beams with External Fibre Reinforced Polymer Reinforcement", *ACI Structural Journal*, 106,1, 2009

[2] Achintha, P.M.M. and Burgoyne, C.J., "Fracture Mechanics of Plate Debonding", *Journal of Composites for Construction*, 12,4, 2008, pp 396-404

[3] Achintha, P.M.M. and Burgoyne, C.J., "Concrete–FRP Interface Fracture Energy", *to be submitted*

[4] Achintha, P.M.M. and Burgoyne, C.J., "Fracture Mechanics of Plate Debonding: Experimental Validation ", *to be submitted*

[5] Fanning, P.J. and Kelly, O., "Ultimate Response of RC beams strengthened with CFRP Plates", *Journal of composites for construction*, , 5, 2, 2001, pp 122-127

[6] Mohamed Ali, M.S., Oehlers, D.J. and Bradford, M.A., "Shear Peeling of Steel Plates Bonded to Tension Faces of RC Beams", *Journal of Structural Engineering*, 127,2, 2001, pp 1453-1459

[7] Quantrill, R.J., Hollaway, L.C. and Thorne, A.M., "Experimental and Analytical Investigation of FRP Strengthened Beam Response", *Magazine of Concrete Research*, 48, 4,1996,pp 331-342

[8] Garden, H.N., Quantrill, R.J., Hollaway, Thorne, A.M. and Parke, G.A.R., "An Experimental Study of the Anchorage Length of Carbon Fibre Composite Plates Used to Strengthen Reinforced Concrete Beams", 12, 4, 1998, pp 203-219